arXiv:1109.1104v1 [cond-mat.mes-hall] 6 Sep 2011

Impurity effects on Fabry-Pérot physics of ballistic carbon nanotubes

F. Romeo[1,2], R. Citro[1,2] and A. Di Bartolomeo[1,2]
[1] *Dipartimento di Fisica "E. R. Caianiello", Università degli Studi di Salerno and* [2] *Institute CNR-SPIN,*
Via Ponte don Melillo, I-84084 Fisciano (Sa), Italy

We present a theoretical model accounting for the anomalous Fabry-Pérot pattern observed in the ballistic conductance of a single-wall carbon nanotubes. Using the scattering field theory, it is shown that the presence of a limited number of impurities along the nanotube can be identified by a measurement of the conductance and their position determined. Impurities can be made active or silent depending on the interaction with the substrate via the back-gate. The conceptual steps for designing a bio-molecules detector are briefly discussed.

Introduction - Single-walled carbon-nanotubes (SWCNTs) are chiral graphene tubules able to show one-dimensional metallic or semiconducting properties depending on their diameter and helicity [1]. Such systems have unique electronic and mechanical properties allowing for the creation of devices useful for fundamental physics applications. Recently a variety of such nanotube-based devices, e.g. single-electron transistors [2], field-effect transistors [3], memory cells [4] and electromechanical devices [5], have been realized. In the non-interacting resonant tunneling regime (i.e. for $U/\Gamma \ll 1$, U and Γ being the Coulomb interaction strength and the tunneling coupling to the leads, respectively), a SWCNT behaves like an almost one dimensional ballistic wire where the quantum interference and the Fabry-Pérot (FP) physics can be tested.

A FP interferometer based on individual SWCNT has been studied in Ref.[6]. In such devices, the nanotube behaves as a coherent electron wave-guide where a resonant cavity is formed within nanotube-electrode interfaces. As a result of the electron scattering at the interfaces, the resonant cavity becomes populated by quasi-bound states formed by the propagating modes (left and right movers) inside the nanotube. The interference between left and right movers can be controlled through a back-gate V_g which produces an electromagnetic phase shift responsible for the FP oscillations of the G-V_g characteristic, G being the differential conductance of the device. Even though the observation of the FP interference is reported in Ref.[6] (see Fig. 1 of that work), the G *vs* V_g curves show additional harmonics compared to the ones expected for an ideal FP interferometer. Recently, these anomalies have been interpreted as the signature of interaction effects [7], while in the original work the magnitude and position of the conductance dips were attributed to disorder effects arising from the underlying substrate or due to intrinsic nanotube defects. The latter hypothesis has never been directly tested and thus a certain part of the experimental interpretation still needs clarification.

Moreover, a recent work[8] showed the possibility to artificially induce defects in SWCNTs by Ar^+ irradiation. Such disordered 1D systems present random pattern of impurities able to confine the electrons which exhibit *particle-in-a-box* physics.

Motivated by the recent interest towards the few-defects physics in SWCNTs and in more controllable systems as e.g. cold atoms systems[9], in this Letter we present a scattering field theory[10] of the FP physics in a one-dimensional wire in the presence of few defects. We would like to account for the anomalies of the G *vs* V_g curves observed in Ref.[6] following the original hypothesis of defect-induced modulation. Our analysis can be relevant to recognize and locate isolated defects in quasi-one-dimensional systems by a simple interferometry experiment.

Model and Formalism - The low energy physics of a metallic impurity-free single-walled carbon nanotube is described by the Hamiltonian:

$$H_0 = -i\hbar v_F \sum_{\sigma,\alpha\in\{L,R\}} \int dx \xi_\alpha : \psi^\dagger_{\alpha\sigma}(x)\partial_x\psi_{\alpha\sigma}(x) : \quad (1)$$

where $\psi_{R(L)\sigma}$ is the right (left) mover electron field with spin $\sigma = \{\uparrow,\downarrow\}$ and chirality $\xi_R = 1$ ($\xi_L = -1$), x is the longitudinal coordinate, while : $\hat{\mathcal{O}}$: stands for the normal ordering of the operator $\hat{\mathcal{O}}$ with respect to the equilibrium state defined by occupied energy levels below the Fermi sea. When the nanotube is put in contact with a metal to form the source/drain electrodes, the sites $x_{1/2}$ (located at nanotube/electrode interfaces) become scattering centers for the electrons and a backscattering occurs. Accordingly, the following term is added to the Hamiltonian of the system[11]:

$$H_c = \sum_{\sigma=\uparrow,\downarrow} \int dx \quad [\Gamma_c(x)\psi^\dagger_{R\sigma}(x)\psi_{L\sigma}(x) + h.c.], \quad (2)$$

where the function $\Gamma_c(x) = 2\hbar v_F \sum_{j=1,2}\delta(x-x_j)\lambda_j$ and λ_j is the scattering strength.

The effect of a back gate on the electron transport can be taken into account by introducing a gate-dependent term:

$$H_g = \sum_\sigma \int_{x_1}^{x_2} dx[eV_g(\rho_{R\sigma} + \rho_{L\sigma})], \quad (3)$$

which depends on the electron densities $\rho_{\alpha\sigma} =: \psi^\dagger_{\alpha\sigma}\psi_{\alpha\sigma}:$ ($\alpha = L, R$ and spin σ) in the channel (i.e. the region

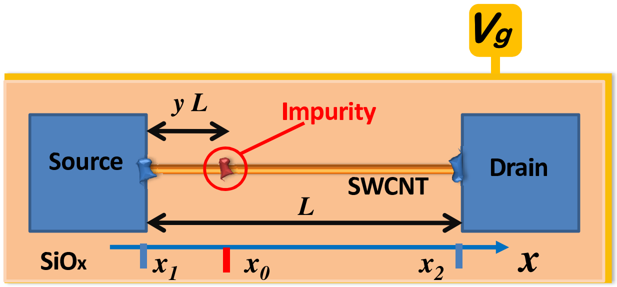

FIG. 1: Carbon nanotube based device described in the main text. The position x_1 and x_2 where the electrodes merge with the nanotube are scattering centers able to couple the left and right movers inside the channel. The back-gate V_g controls the electromagnetic phase kept by the electrons interfering in the system, while the presence of an impurity in x_0 affects the Fabry-Pérot physics introducing additional harmonics to the G *vs* Φ_g relation.

$x_1 < x < x_2$) and the electrostatic potential V_g of the back-gate.

The presence of an impurity with effective size l_s comparable to the lattice constant a_0 along the nanotube affects the electron transport causing an additional scattering at $x_0 \in [x_1, x_2]$ which is described by the Hamiltonian:

$$H_I = \sum_{\sigma=\uparrow,\downarrow} \int dx \quad [\Gamma_I(x)\psi^\dagger_{R\sigma}(x)\psi_{L\sigma}(x) + h.c.], \tag{4}$$

where $\Gamma_I(x) = 2\hbar v_F \delta(x - x_0)\lambda_0$.

To determine the differential conductance G of the device a scattering field theory *à la* Büttiker [10] can be implemented, while the space-time dependent electron fields can be obtained using the equation of motion (EOM) method. In absence of impurities, i.e. when $\lambda_0 \to 0$, the dynamics of the electron field $\psi_{\alpha\sigma}(x)$ far from the contacts is described by the equation

$$[\partial_t + \xi_\alpha v_F \partial_x - \frac{eV_g}{i\hbar}\Phi(x)]\psi_{\alpha\sigma}(x) = 0, \tag{5}$$

where $\Phi(x)$ is a step-like function which takes value 1 in the channel, i.e. for $x_1 < x < x_2$, and 0 elsewhere. The scattering fields solving (5) are written below:

$$\hat\psi_{R\sigma}(x,t) = \frac{e^{ik_E x - iEt/\hbar}}{\sqrt{2\pi\hbar v_F}} \times \begin{array}{ll} \hat a_{R\sigma}(E) & x < x_1 \\ e^{-i\frac{eV_g}{\hbar v_F}}\hat c_{R\sigma}(E) & x_1 < x < x_2 \\ \hat b_{R\sigma}(E) & x > x_2 \end{array} \tag{6}$$

and

$$\hat\psi_{L\sigma}(x,t) = \frac{e^{-ik_E x - iEt/\hbar}}{\sqrt{2\pi\hbar v_F}} \times \begin{array}{ll} \hat b_{L\sigma}(E) & x < x_1 \\ e^{i\frac{eV_g}{\hbar v_F}}\hat c_{L\sigma}(E) & x_1 < x < x_2 \\ \hat a_{L\sigma}(E) & x > x_2 \end{array} \tag{7}$$

where $k_E = E/(\hbar v_F)$. The interaction of the electrons with the delta-like potentials mimicking the contacts interface is described by imposing the appropriate boundary conditions of the scattering fields describing the incoming and the outgoing particles. The $\mathcal{S}$-matrix relates the scattering fields according to $\hat{\mathbf{b}} = \mathcal{S}\hat{\mathbf{a}}$, where the outgoing (incoming) field vector is given by $\hat{\mathbf{b}} = (\hat b_{L\uparrow}, \hat b_{L\downarrow}, \hat b_{R\uparrow}, \hat b_{R\downarrow})^t$ ($\hat{\mathbf{a}} = (\hat a_{R\downarrow}, \hat a_{R\uparrow}, \hat a_{L\downarrow}, \hat a_{L\uparrow})^t$). The current operators within the scattering formalism can be written as follows:

$$\begin{aligned} \hat J_L(t) &= -(|e|/h)\sum_{i=1,2}[\hat a_i^\dagger(t)\hat a_i(t) - \hat b_i^\dagger(t)\hat b_i(t)] \\ \hat J_R(t) &= (|e|/h)\sum_{i=3,4}[\hat a_i^\dagger(t)\hat a_i(t) - \hat b_i^\dagger(t)\hat b_i(t)]. \end{aligned} \tag{8}$$

Considering that $\hat a_i(t) = \int dE e^{-iEt/\hbar}\hat a_i(E)$ and using the quantum average $\langle \hat a_j^\dagger(E)\hat a_i(E')\rangle = \delta_{ij}\delta(E - E')f_i(E)$ (f being the Fermi function) for the incoming fields, one obtains the linear response charge current J_L measured in the left lead:

$$J_L = -(e^2/h)\int d\xi \sum_{i,j}\Big[\delta_{ij} - |\mathcal{S}_{ij}(\xi)|^2\Big](\partial_\xi f(\xi))_{eq} V_j, \tag{9}$$

where the voltage bias $V_j = V$ ($-V$) if $j = 1, 2$ ($j = 3, 4$), $i \in \{1, 2\}$, $j \in \{1, ..., 4\}$, while the indices (i, j) are defined in [12]. Starting from Eq.(9) the differential conductance $G = \partial_V J_L$ is easily obtained. In the case of a single delta-like scatterer in the wire (mimicking the contact interface or an impurity) the only nonvanishing elements of the scattering matrix are: $\mathcal{S}_{12} = \mathcal{S}_{21} = \mathcal{S}_{34} = \mathcal{S}_{43} = -2i\gamma/(1+\gamma^2)$, $\mathcal{S}_{14} = \mathcal{S}_{41} = \mathcal{S}_{23} = \mathcal{S}_{32} = (1-\gamma^2)/(1+\gamma^2)$, where $\gamma = \lambda_j$. The formalism described so far can be easily generalized to the n-impurities case by composition law of scattering matrices as given e.g. in Ref.[13]. In this way the charge transport through a SWCNT can be studied in the quasi-ballistic regime. Below we focus on the case of three scatterers in the zero-temperature limit.

Results - Our approach is employed to analyze the experimental data presented in Ref.[6] where the FP physics has been shown by the measure of the differential conductance of a single-walled carbon nanotube. For an open ballistic channel the zero-bias conductance is NG_0 where $G_0 = e^2/h$ is the quantum of conductance and N the number of modes. Thus one expects that in the absence of scattering events the ballistic conductance of a SWCNT is $4e^2/h$; however in the presence of non-ideal contacts or of the interaction with substrate impurities, back-scattering events reduce the transmission probability of the system. In order to understand such effects on the differential conductance we take $\lambda_0 = \lambda_1 = \lambda_2 = \gamma$ and focus on the high transparency limit (i.e. $\gamma \ll 1$) which seems to be appropriate for the experiment reported in Ref.[6]. Under these assumptions the analytical expression of the conductance to the order γ^2 is

$$G/G_0 \;\simeq\; 4-16\gamma^2\Big[3+2\cos(2\Phi_g)+ \qquad (10)$$
$$+\;\; 2\cos(2\Phi_g(y-1))+2\cos(2\Phi_g y)\Big]+\mathcal{O}(\gamma^4),$$

where the gate-induced electromagnetic phase is defined as $\Phi_g = eV_gL/(\hbar v_F)$, while y is a dimensionless factor measuring the position of the impurity normalized to the total length L of the nanotube. Eq.(10) shows that the FP physics is controlled by the back-gate V_g. Differently from the impurity-free case, the gate-induced oscillations of $G(\Phi_g)$ include the terms $\cos(2\Phi_g\beta)$, $\beta \in \{y, y-1\}$, which collapse into the usual $\cos(2\Phi_g)$ when $\beta = 0$ or 1, i.e. for an impurity residing on the left or the right contact. The properties reported above imply that a carbon-nanotube with an impurity behaves like a sequence of two FP interferometers of length yL and $(1-y)L$, respectively. Since a sequence of n FP interferometers can be used to design systems with special optical properties, one can expect that controlling the introduction of impurities in ballistic nanotubes can be useful in obtaining quantum devices with controllable electronic properties. A work on the effects of defects produced in CNT by means of Ar^+ irradiation recently appeared[8], even though only random patterns of impurities were obtained.

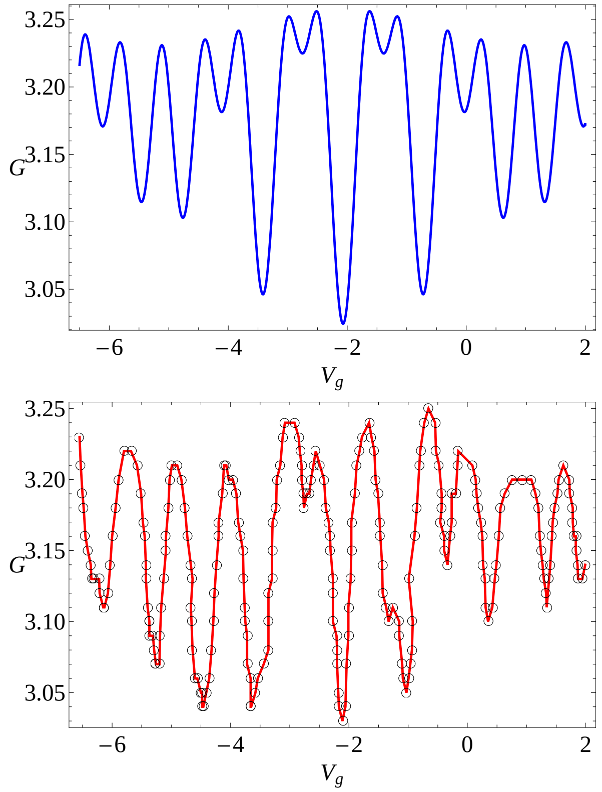

FIG. 2: Upper panel: Differential conductance G (in unit of e^2/h) *vs* V_g using the following parameters: $\gamma = 0.05$, $y = 0.4465$, $\Phi_g = \Omega_V(V_g - V_g^0)$, $\Omega_V = 4.65/V$, $V_g^0 = -2.07$ V, $z = 0.057$. Lower panel: Experimental data as extracted by Fig.1 of Ref.[6].

In Fig.2 we compare our results with the FP pattern observed in Fig.1 of Ref.[6] and reproduced in the lower panel of Fig.2. In order to achieve a quantitative comparison with experimental data, we introduce the contacts conductance, i.e. G_1 and G_2, which takes into account the renormalization of the electrons tunneling in the nanotube, while the conductance G of the whole system is obtained by the composition law:

$$G = \frac{G_{NT}}{1+zG_{NT}}, \qquad (11)$$

where G_{NT} is the differential conductance (in units of $G_0 = e^2/h$) of the SWCNT as computed using the previous scattering model, while z is the contacts transparency, $z = G_0(G_1+G_2)(G_1G_2)^{-1}$. In the upper panel of Fig.2 we report the differential conductance G (in unit of e^2/h) *vs* V_g using the following set of parameters: $\gamma = 0.05$, $y = 0.4465$, $\Phi_g = \Omega_V(V_g - V_g^0)$, $\Omega_V = 4.65/V$, $V_g^0 = -2.07$ V, $z = 0.057$. By comparing the upper and lower panel of Fig.2 the modulation of the maxima and minima, the oscillation period and the general qualitative features of the experimental G *vs* V_g curve are correctly reproduced. As for the fitting parameters, $z = 0.057$ corresponds to a contact conductance $G_1 \simeq G_2 = G_c \approx 30e^2/h$. This value is consistent with the one usually found in carbon-based mesoscopic systems [14]. The other fitting parameter is y which fixes the position of the scattering center at distance $0.447L$ from the left lead (see Fig.1), while the scattering strength is $\gamma = 0.05$, which is quite weak and consistent with the high value of the differential conductance of the device. Let us note that in general the scattering strength of the impurities depends on the back-gate V_g [15], and thus by varying V_g one can observe the activation (switching off) of an impurity previously silent (active). This phenomenon can be detected by the deformation of the interference pattern and the appearance of additional unusual features. In the above analysis the relation between the electromagnetic phase Φ_g and the back-gate V_g has been taken of the form $\Phi_g = \Omega_V(V_g - V_g^0)$ to describe the linear electromagnetic response of the substrate to the applied potential V_g around the working point defined by V_g^0. Indeed, $V_g - V_g^0$ represents an effective potential that takes into account charge trapping at the oxide-nanotube interface. When the parameter Ω_V is compared to $eL/(\hbar v_F)$, i.e. the value of Φ_g/V_g, the relation $\Omega_V = eL\eta/(\hbar v_F)$ is correctly found. The dimensionless factor $\eta \approx 10^{-2}$ is known as gate efficiency[16] and represents the fraction of applied back-gate voltage felt by the SWCNT electrons. In Fig.3 we report the density plot of the differential conductance G (in unit of e^2/h) in the plane (V_g, y) obtained by fixing the model parameters as done in Fig.2 and varying the impurity position. As evident from the analysis

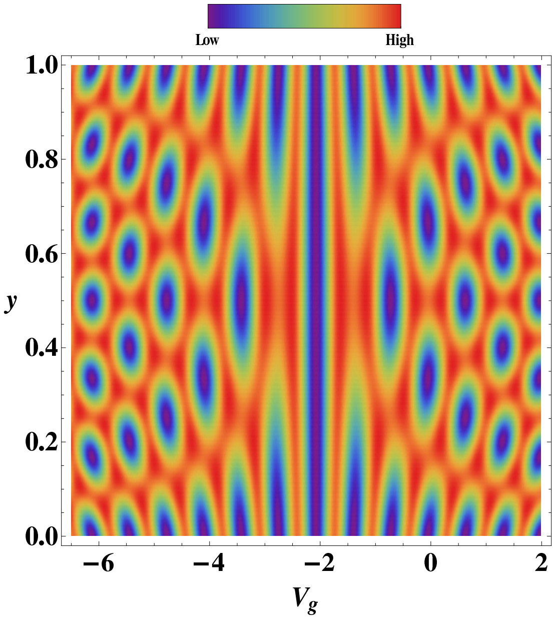

FIG. 3: Density plot of the differential conductance G (in unit of e^2/h) in the plane (V_g, y) obtained by fixing the model parameters as done in Fig.2. One can notice the modulation of the FP pattern as a function of the impurity position y.

of that figure, the FP pattern is strongly affected by the impurity position y. The impurities located close to the leads, i.e. for $0 < y < 0.05$ or $0.95 < y < 1$, only cause a lowering of the effective contacts transparency without introducing important changes in the FP curves. Impurities located in the channel, i.e. for $0.2 < y < 0.8$, induce modifications in the G *vs* V_g curves (as the location and amplitude of the dips) and thus their presence can be easily detected. The mentioned properties could also be useful to design electrically-readable sensors where a certain number of sites along the nanotube behave like *instructed impurities*. Such impurities can be of two types, active or silent, depending on the interaction with the environment (chemical or biological)[17]. Finally we point out that the results shown in Fig.3 are similar to the ones obtained in Ref.[8] where the atomic structure and chirality of the SWCNT were fully taken into account.

Conclusions - We presented a scattering theory *à la* Büttiker accounting for the FP pattern measured in ballistic SWCNTs with a limited number of impurities. Using our theoretical model, we were able to reproduce the experimental data reported in Ref.[6] offering a quantitative test for an impurity-modulated FP pattern in the G-V_g characteristic. We provided an alternative explanation of the experimental data compared to the ones given in Ref.[7]. Thus, the present work adds supplementary information useful in understanding interferences effects in carbon-based resonant cavities. On the pratical point of view, the sensible dependence of the differential conductance on the impurities position could be a useful ingredient in designing biological sensors.

Acknowledgements - The authors wish to acknowledge D. Bercioux for helpful discussions and Prof. H. Park for having given access to the experimental data.

[1] S. Iijima, Nature (London) **354**, 56 (1991); Noriaki Hamada, Shin-ichi Sawada, and Atsushi Oshiyama, Phys. Rev. Lett. **68**, 1579 (1992); C. Schönenberger, Semicond. Sci. Technol. **21**, S1-S9 (2006)

[2] M. Bockrath *et al.*, Science **275**, 1922 (1997); S. J. Tans *et al.*, Nature **386**, 474 (1997).

[3] S. J. Tans, R. M. Verschueren, C. Dekker, Nature **393**, 49 (1998); R. Martel *et al.*, Appl. Phys. Lett. **73**, 2447 (1998); A. Di Bartolomeo, M. Rinzan, A. K. Boyd, Y. Yang, L. Guadagno, F. Giubileo, and P. Barbara, Nanotechnology **21**, 115204 (2010)

[4] A. Di Bartolomeo, Y. Yang, M. B. M. Rinzan, A. K. Boyd, P. Barbara, Nanoscale Res. Lett. **5**, 1852 (2010)

[5] T. W. Tombler *et al.*, Nature **405**, 769 (2000); T. Rueckes *et al.*, Science **289**, 94 (2000)

[6] W. Liang, M. Bockrath, D. Bozovic, J. H. Hafner, M. Tinkham, and H. Park, Nature **411**, 665 (2001)

[7] Claudia S. Peça, Leon Balents, and Kay Jörg Wiese, Phys. Rev. B **68**, 205423 (2003)

[8] G. Buchs, D. Bercioux, P. Ruffieux, P. Gröning, H. Grabert, and O. Gröning, Phys. Rev. Lett. **102**, 245505 (2009); D. Bercioux, G. Buchs, H. Grabert, and O. Gröning, Phys. Rev. B **83**, 165439 (2011)

[9] J. Catani *at al.*, `arXiv: 1106.0828v1` (2011)

[10] M. Büttiker, Phys. Rev. B **46**, 12485 (1992)

[11] Note that we neglect the renormalization of particles incoming from the electrode due to the metal-nanotube interaction, that will be taken into account in the calculation of G afterwards (see Eq. (11)).

[12] Notice that for the outgoing states the indices of the scattering matrix have to be interpreted as follows: $i = 1 \rightarrow (L, \uparrow)$, $i = 2 \rightarrow (L, \downarrow)$, $i = 3 \rightarrow (R, \uparrow)$, $i = 4 \rightarrow (R, \downarrow)$. Concerning the incoming states the notation becomes: $i = 1 \rightarrow (R, \downarrow)$, $i = 2 \rightarrow (R, \uparrow)$, $i = 3 \rightarrow (L, \downarrow)$, $i = 4 \rightarrow (L, \uparrow)$.

[13] T. Ouisse, *Electron Transport in Nanostructures and Mesoscopic Devices: An Introduction*, (John Wiley and Sons Inc, Hoboken, NJ, 2008); see chap. 4.

[14] Seong Chu Lim *et al.*, Appl. Phys. Lett. **95**, 264103 (2009)

[15] M. Bockrath *et al.*, Science **291**, 283 (2001)

[16] F. Léonard, *The Physics of Carbon Nanotube Devices*, (William Andrew Publishing , Norwich, NY, 2009)

[17] See for instance Jing Kong *et al.*, Science **287**, 622 (2000)